AP2XII-2 coordinates transcriptional repression for *Toxoplasma gondii* sexual commitment

Sandeep Srivastava[1#], Michael J. Holmes[1#], Michael W. White[3],
William J. Sullivan, Jr[1-2*]

[1]Department of Pharmacology & Toxicology, [2]Department of Microbiology & Immunology, Indiana University School of Medicine, Indianapolis, 46202, Indiana
[3]Department of Global Health, University of South Florida, Tampa, Florida

Running title: AP2XII-2 role in *Toxoplasma* sexual development

[#] Equal contribution
*Corresponding author:
William J. Sullivan, Jr.
Showalter Professor
Indiana University School of Medicine
635 Barnhill Drive
MS A418C
Indianapolis, IN 46202
(317) 274-1573; wjsulliv@iu.edu

ABSTRACT

Toxoplasma gondii is a widespread protozoan parasite that has significant impact on human and veterinary health. The parasite undergoes a complex life cycle involving multiple hosts and developmental stages. How *Toxoplasma* transitions between life cycle stages is poorly understood, yet central to controlling transmission. Of particular neglect are the factors that contribute to its sexual development, which takes place exclusively in feline intestines. While epigenetic repressors have been shown to play an important role in silencing spurious gene expression of sexually committed parasites, the specific factors that recruit this generalized machinery to the appropriate genes remains largely unexplored. Here, we establish that a member of the AP2 transcription factor family, AP2XII-2, is targeted to genomic loci associated with sexually committed parasites along with the epigenetic regulators of transcriptional silencing, HDAC3 and MORC. Despite widespread association with gene promoters, AP2XII-2 is required for silencing of relatively few genes. Using CUT&Tag methodology, we identify two major genes associated with sexual development downstream of AP2XII-2 control, AP2X-10 and the amino acid hydroxylase AAH1. Our findings show that AP2XII-2 is a key contributor to the gene regulatory pathways modulating *Toxoplasma* sexual development.

IMPORTANCE

Toxoplasma gondii is a parasite that undergoes its sexual stage exclusively in feline intestines, making cats a major source of transmission. A better understanding of the proteins controlling the parasite's life cycle stage transitions is needed for the development of new therapies aimed to treat toxoplasmosis and transmission of the infection. Genes that regulate the sexual stages need to be turned on and off at the appropriate times, activities that are mediated by specific transcription factors that recruit general machinery to silence or activate gene expression. In this study, we identify a transcription factor called AP2XII-2 as being important for repression of a subset of sexual stage genes, including a sexual stage-specific AP2 factor (AP2X-10) and a protein (AAH1) required to construct the infectious oocysts expelled by infected cats.

INTRODUCTION

The ubiquitous parasite *Toxoplasma gondii* (phylum Apicomplexa) infects warm-blooded animals the world over, including approximately one in three people (1). After an initial acute phase of infection by tachyzoites, the parasites redistribute within the solid organs of the infected host and reside as bradyzoites in latent tissue cysts that appear impervious to the immune response and currently available treatments (1). Persistence within the host makes *Toxoplasma* an opportunistic infection in those with compromised immune systems (1). Upon immune suppression, latent bradyzoite stage parasites reconvert into rapidly growing tachyzoites, causing severe tissue destruction that can threaten the life of the infected individual (1).

Given the importance of interconversion between tachyzoites and bradyzoites to disease progression, the molecular mechanisms governing this stage transition have received a great deal of attention (2). The conversion of tachyzoites to bradyzoites requires extensive reprogramming of gene expression at multiple levels, directed in part by chromatin remodeling histone acetyltransferases and deacetylases that are recruited to specific gene loci through their interactions with sequence-specific transcription factors (3, 4). In support of this, members of the AP2 transcription factor family have been found to associate with a cadre of histone modifying complexes including GCN5b/ADA2a and HDAC3/MORC (5, 6). AP2 transcription factors harbor a plant-like DNA-binding domain and have been implicated in contributing to the regulation of gene expression in apicomplexan parasites (7).

In contrast, our understanding of the molecular mechanisms governing the rewiring of gene expression during *Toxoplasma* sexual development is far less developed, largely due to a lack of model systems. This is despite evidence showing that ingestion of the ultimate product of *Toxoplasma* sexual reproduction, sporulated oocysts, accounts for a substantial portion of worldwide human infections and mass outbreaks of acute toxoplasmosis (8, 9).

The early stages of *Toxoplasma* sexual development occur in the intestinal lining of cats. Upon ingestion by the feline, the parasites invade the intestinal enteroepithelial cells and undergo several rounds of schizogonic replication to produce merozoites (10). Successive rounds of schizogony have been subcategorized into types A-E of the enteroepithelial stage. These pre-sexual stages then undergo gametocytogenesis, ultimately producing motile male microgametes and intracellular female macrogametes. After fertilization, up to a billion immature oocysts are expelled with the cat's feces (11). Upon exposure to the air, the oocysts sporulate and become capable of transmitting infection (10).

It has recently been shown that transcriptional repression mediated by the HDAC3/MORC complex plays an important role in preventing the aberrant expression of genes normally restricted to the sexual stages in felids (6). The HDAC3/MORC complex associates with at least 11 AP2 family transcriptional regulators (6, 12), suggesting that these factors mediate targeted silencing of felid-specific developmental gene expression, as proposed for bradyzoite formation (4).

We initially found AP2XII-2 to be in association with AP2IX-4, a transcriptional repressor that helps coordinate bradyzoite formation (12, 13). We then reported that

AP2XII-2 is required for proper progression of parasites through the S-phase of the tachyzoite cell cycle and that knockdown of AP2XII-2 increased frequency of bradyzoite formation *in vitro* (12). We and others have also reported the association between the HDAC3/MORC complex and AP2XII-2 (6, 12), suggesting that this AP2 family member controls the transcriptional repression of certain genes. However, the specific genes regulated by AP2XII-2 remained unexplored.

To better understand the role of AP2XII-2 in *Toxoplasma* biology, we profiled the genome-wide chromatin-binding sites of AP2XII-2. By adopting Cleavage Under Targets and Tagmentation (CUT&Tag) for use in *Toxoplasma*, we found find a high degree of overlap between AP2XII-2 and HDAC3/MORC target genes. Using a transcriptomics approach, we also found that AP2XII-2 controls the expression of a subset of HDAC3/MORC-target genes, including some that are restricted to the sexually-committed developmental stages such as AP2X-10 and the aromatic amino acid hydroxylase, AAH1. Our results indicate that AP2XII-2 helps coordinate recruitment of the HDAC3/MORC complex to specific gene loci to repress developmentally-controlled genes.

RESULTS AND DISCUSSION

AP2XII-2 shows widespread occupancy at gene promoters and high degree of overlap with the HDAC3/MORC complex

To identify genes that are direct targets of AP2XII-2 in tachyzoites, we applied the CUT&Tag method (14) to profile the genomic loci bound by the factor. To pulldown

124 AP2XII-2 for CUT&Tag, we took advantage of a parasite clone we made previously in
125 ME49 strain that expresses an HA-tagged version of the endogenous protein (12).
126 Results showed that AP2XII-2-associated regions are widespread across the parasite
127 genome, displaying a total of 5,527 peaks associated with 3,939 genes (Table S1; Fig.
128 1A). Consistent with its putative role as a transcriptional regulator, AP2XII-2 is located
129 near the transcriptional start site of protein coding genes (Fig. 1B).

130 Previous reports have demonstrated that AP2XII-2 is a member of the multi-
131 component HDAC3/MORC complex, which silences genes by inducing heterochromatin
132 formation (6, 12). To corroborate this association, we re-analyzed the existing HDAC3
133 and MORC ChIPseq data (6) to determine the overlap between HDAC3, MORC, and
134 AP2XII-2 localization genome-wide (Table S1). Like AP2XII-2, both HDAC3 and MORC
135 are enriched at the transcriptional start site of protein coding genes (Fig. 1B). Just over
136 80% of AP2XII-2 enriched regions overlapped with HDAC3 and/or MORC enriched
137 peaks (Fig. 1C). Additionally, over 85% of genes associated with AP2XII-2 were also
138 bound by HDAC3 and/or MORC with a clear plurality of all identified genes bound by
139 the three proteins (Fig. 1D). Given that AP2 domains bind distinct DNA motifs and that
140 HDAC3 and MORC lack DNA binding domains (15, 16), combined with the previous
141 observation that they operate within a shared complex (6, 12), the high degree of
142 coordination between AP2XII-2, HDAC3, and MORC binding sites strongly suggests
143 that AP2XII-2 is responsible for recruiting the HDAC3/MORC complex to repress
144 specific genes.
145

146 **Loss of AP2XII-2 disrupts a small subset of protein coding transcripts in**
147 **tachyzoites**

148 Given that AP2XII-2 associates with a large number of gene promoters and likely
149 directs transcriptional silencing through the HDAC3/MORC complex, we wanted to
150 assess the consequences of AP2XII-2 depletion on transcriptional regulation. To
151 maximize the robustness of this experiment, we compared the response to AP2XII-2
152 depletion in both type I (RH strain) and type II (ME49 strain) backgrounds using
153 parasites we made in a previous study (12). These parasites express endogenous
154 AP2XII-2 tagged at its C-terminus with a dual tag comprised of an HA epitope and an
155 auxin-inducible degron (AID). TheAP2XII-2^{AID-HA} protein in both strains was degraded to
156 undetectable levels within 24 hours of adding 500 μM indole-3-acetic acid (IAA) to the
157 culture media (Fig. 2A).

158 Using these conditions, comparative RNA sequencing (RNAseq) analyses
159 revealed that the loss of AP2XII-2 in tachyzoites led to dysregulation of mRNA levels for
160 a modest number of transcripts in both the RH and ME49 genetic backgrounds (Table
161 S2). In RH parasites lacking AP2XII-2, 66 genes were significantly upregulated and 39
162 genes were downregulated at least 1.5 fold (Fig. 2B). Similarly, in ME49 parasites, 143
163 genes were significantly upregulated and 120 genes were downregulated 1.5 fold
164 following depletion of AP2XII-2 (Fig. 2C). The majority of the dysregulated genes in RH
165 strain were also dysregulated in ME49 strain, indicating a high degree of concurrence
166 between strains (Fig. 2D). Surprisingly, there was no correlation between the direction
167 of transcriptional dysregulation and AP2XII-2 gene occupancy as determined by
168 CUT&Tag (Fig. 2E). This observation likely speaks to the complexity of gene regulation

169 in *Toxoplasma*, which can involve multiple AP2 factors and chromatin remodeling
170 machinery. Depletion of a single factor like AP2XII-2 may not be sufficient to
171 significantly disrupt expression of most genes in the network. Since AP2XII-2 was also
172 found to interact with AP2IX-4 (12), our observations here may point to a model where
173 AP2 family members cooperatively bind for efficient HDAC3/MORC recruitment to
174 specific gene loci.

175 Since AP2XII-2 is a cell cycle regulated factor with expression peaking during the
176 S/M phases (12, 17), we assessed whether the dysregulated genes were also subject to
177 cyclic control. Using the cell cycle microarray data available on ToxoDB.org (17, 18), we
178 determined the average cell cycle profiles for the genes that were up- or downregulated
179 in response to AP2XII-2 depletion and compared them to the cell cycle pattern exhibited
180 by AP2XII-2 (Fig. 2F). Downregulated genes tended to be cell cycle regulated with a
181 valley of expression that spans mid-G1 phase, in line with our previous observation that
182 AP2XII-2 depletion delays the cell cycle after centrosome duplication (12). The
183 expanded G1 phase occupancy induced by AP2XII-2 depletion may point to a linkage
184 between transcriptional repression of AP2XII-2 target genes and the cell cycle. Despite
185 not displaying cell cycle regulation, the upregulated genes were expressed at lower
186 robust multichip average (RMA) expression values. The relatively low abundance of
187 these genes in tachyzoites could indicate that they are normally subjected to
188 transcriptional repression. Given the association of AP2XII-2 with the HDAC3/MORC
189 transcriptional repression complex (6, 12), we suspected that these upregulated genes
190 could be subject to regulation by AP2XII-2 via recruitment of HDAC3/MORC.
191

192 **Loss of AP2XII-2 increases expression of genes normally restricted to latent and**
193 **sexually committed parasites**

194 To identify genes that are most likely to be direct targets of the AP2XII-2-directed
195 HDAC3/MORC complex, we looked for genes that were upregulated in 1) either ME49
196 or RH strain parasites upon AP2XII-2 depletion, 2) after 24 hours of MORC depletion
197 (Fig. S1A), and 3) after 18 hours incubation with the HDAC3 inhibitor FR235222 (Fig.
198 S1B). These latter two criteria were assessed using publicly available data and were
199 also generated from a type II parasite strain (Table S3) (6). In addition, we verified that
200 each gene's promoter was occupied by AP2XII-2, HDAC3, and MORC. Five gene
201 accession entries met this stringent filtering criteria (Table 1).

202

203 **Table 1. Genes occupied by AP2XII-2, HDAC3, and MORC that are consistently**
204 **upregulated upon their depletion or inhibition.**

		AP2XII-2 depletion			
Gene ID	Product Description	ME49[a]	RH[a]	MORC[a]	HDAC3[a]
TGME49_212710	phenylalanine-4-hydroxylase (F4H)	2.18	0.86	4.29	3.74
TGME49_287510	aromatic amino acid hydrolase (AAH1)	0.58	1.40	4.91	3.22
TGME49_318750	deoxyribose-phosphate aldolase (TgDPA)	1.82	1.30	1.39	1.40
TGME49_215340	AP2X-10 (fragment)	1.16	1.01	5.19	3.57
TGME49_215343	hypothetical protein (AP2X-10 fragment)	1.13	1.00	5.27	3.45

205 [a] $\log_2$FC values

206

207 The auxin-induced depletion of MORC as well as inhibition of HDAC3 in
208 tachyzoites induced upregulation of bradyzoite-specific genes as well as genes

209 associated with sexual stages (6, 19). Notably, when assessing the degree of
210 dysregulation for the genes outlined in Table 1, the effect was more pronounced for
211 MORC and HDAC3 than for AP2XII-2 depletion. This observation is consistent with a
212 model whereby multiple AP2 family members cooperatively recruit the HDAC3/MORC
213 complex to genomic loci.

214 It has been proposed that parasites must pass through the bradyzoite stage
215 before initiating sexual commitment (6, 20). Our analysis (Table I) identified a single
216 bradyzoite-specific gene, TgDPA (21), to be reliably upregulated under all three
217 treatments that were assessed, strongly suggesting that its expression is controlled by
218 an AP2XII-2-directed HDAC3/MORC complex. The role that TgDPA plays in bradyzoite
219 biology and their potential commitment to sexual development remain to be elucidated.

220 Interestingly, the AP2 family member AP2X-10, whose current fragmented gene
221 annotation incorrectly assigns the gene to both TGME49_215340 and
222 TGME49_215343, is upregulated when either AP2XII-2, MORC, or HDAC3 is impaired
223 independent of parasite strain (Table 1). AP2X-10 expression has been noted to be
224 restricted to the enteroepithelial and oocyst stages; it is the most abundant of all AP2
225 factors in oocysts, being expressed at the 96th percentile (22-24). Seventeen AP2 family
226 members have been proposed to act downstream of the HDAC3/MORC complex to
227 regulate various developmental trajectories, with AP2X-10 predicted to guide micro-
228 and/or macrogamete development (6). Our present study is consistent with AP2XII-2
229 coordinating the repression of AP2X-10, placing the former above AP2X-10 in a
230 transcriptional regulatory cascade that contributes to the coordination of *Toxoplasma*

231 sexual development. Future studies to determine the genes directly controlled by AP2X-
232 10 and clarify its role in sexual development are warranted.
233
234 **AAH family gene organization**
235 Two aromatic amino acid hydroxylase enzymes, AAH1 and F4H, are not only
236 counted amongst the highest upregulated genes upon AP2XII-2, MORC, and HDAC3
237 inhibition (Table 1), but have also been reported to be important for oocyst maturation
238 (25). Interestingly, we found that F4H was upregulated in ME49 but not RH strain, AAH1
239 showed the opposite trend (Table 1). These observations prompted us to further
240 examine the entire aromatic amino acid hydroxylase family in *Toxoplasma*, which
241 consists of three annotated members, TGME49_287510 (AAH1), TGME49_212740
242 (AAH2), and TGME49_212710 (F4H).
243 Previous reports have indicated that the current ME49 genome assembly
244 available on ToxoDB.org has incorrectly fused a tandem repeat of the AAH2 gene (25,
245 26). Before proceeding with our analysis, we had to ensure the fidelity of the AAH2
246 gene sequence. To that end, we compared the ME49 genome assembly with the RH88
247 assembly since the former was generated using short read sequencing technology,
248 which can have difficulty with repetitive regions (Fig. 3A). The RH88 genome was
249 constructed based on long read sequencing technology, which is better at determining
250 overall genome architecture (27). This comparison revealed that indeed two members
251 of the AAH family should appear on chr V of the ME49 genome, spaced apart by
252 unplaced contigs KE139705 and KE139818 (Fig. 3A).

253 The three ME49 members of the AAH family share over 99.4% identity at the
254 nucleotide level in their coding sequences (Fig. 3B), suggesting that the vast majority of
255 RNAseq reads mapping to the CDS region would have been assigned to all AAH genes
256 indiscriminately; this spurious read assignment may indicate that a putative strain-
257 specific upregulation of AAH1 or F4H could occur by chance (Table 1). Given the high
258 degree of sequence identity between each AAH family member, we examined their
259 flanking sequences to differentiate them. AAH1 and AAH2 have unique 3'end flanking
260 sequences (Fig. 3C), however the unplaced contig KE139818 abruptly ends, leaving the
261 annotated F4H gene (TGME49_212710) without a 3'UTR sequence (Fig. 3D). Analysis
262 of the unique regions flanking the 5' and 3' ends of the AAH family by sequence
263 alignment comparison with the RH88 genome architecture allowed us to place AAH1
264 and AAH2 onto chr V and determine that F4H and AAH2 are likely the same gene (Fig.
265 3A). However, it should be noted that a previously conducted copy number variant
266 analysis of the AAH family in *Toxoplasma* indicated that ME49 parasites harbor three
267 copies of AAH genes whereas type I parasites encode only two (25). We were unable to
268 map the location of the additional AAH family member with our strategy of comparing
269 ME49 and RH genome architectures.
270
271 **Depletion of AP2XII-2 de-represses AAH1 but not AAH2**
272 To distinguish which AAH family member(s) are upregulated upon AP2XII-2
273 depletion, we endogenously tagged AAH1 and AAH2 with MYC epitopes at their C-
274 termini in ME49 AP2XII-2^{AID-HA} parasites. The tagging of these genes was confirmed by
275 verifying successful recombination at each genetic locus by PCR analysis (Fig. S2). In

276 untreated parasites, AAH1^{MYC} was not detectable by western blotting whereas AAH1^{MYC}
277 appeared at the expected size of 62 kDa upon IAA-induced loss of AP2XII-2 (Fig. 4A).
278 Expression of AAH2^{MYC} was not seen under either condition (Fig. 4B).

279 Neither AAH family member is typically expressed in asexual parasites (26),
280 suggesting that they are maintained in a transcriptionally repressed state in non-
281 sexually committed parasites. Our results suggest that AAH genes may be regulated by
282 different HDAC3/MORC-AP2 complexes, with AP2XII-2 directing the silencing of AAH1
283 but not AAH2. However, we cannot rule out the possibility that AAH1 and AAH2 have a
284 parasite strain specific dependence on AP2XII-2. Since parasites lacking AAH1 have a
285 severe defect in infection of the cat intestine and oocyst production (25), we propose
286 that AP2XII-2 is a key factor required for completion of *Toxoplasma* sexual
287 reproduction.

288 We next examined AAH1 expression by immunofluorescence assay (IFA) and
289 found AAH1^{MYC} to be localized around the nuclei of tachyzoites only upon AP2XII-2
290 depletion (Fig. 4C). This staining pattern is reminiscent of the *Toxoplasma*
291 mitochondrion. To further characterize AAH1^{MYC} localization, we co-stained AP2XII-2^{AID-}
292 ^{HA} knockdown parasites with antibodies to the F_1B ATPase mitochondrial marker (28)
293 and the MYC epitope tag, which confirmed the co-localization of AAH1^{MYC} with the
294 mitochondrion in tachyzoites (Fig. 4D).

295 The AAH family of enzymes is responsible for converting phenylalanine to
296 tyrosine and tyrosine to 3,4-dihydroxy-L-phenylalanine (L-DOPA) (29). The later
297 compound is a precursor for the formation of di-tyrosine protein crosslinks that are
298 thought to play a critical structural role in *Toxoplasma* oocyst wall integrity and formation

299 (25). Given the role that AAH family enzymes play in ensuring oocyst development and
300 wall integrity, we were surprised to see AAH1 localized to the parasite mitochondrion.
301 Interestingly, a previous report demonstrated that AAH2 overexpression in bradyzoites
302 gave rise to a staining pattern consistent with mitochondrial localization (26), suggesting
303 that the mitochondrion might act as a hub for AAH enzymatic activity. Future studies
304 using bona fide sexually-committed parasites are needed to verify this possibility.
305

306 **Conclusion**

307 We have determined that in addition to affecting tachyzoite cell cycle progression
308 (12), AP2XII-2 also plays a role in coordinating *Toxoplasma* sexual development. This
309 may indicate that AP2XII-2 plays different roles in different developmental stages or
310 may suggest that the commitment to sexual development is a cell-cycle dependent
311 phenomenon as has been demonstrated for the tachyzoite to bradyzoite transition (7,
312 30). Consistent with this model, either inhibition of HDAC3 or MORC depletion also stall
313 cell cycle progression and lead to increased bradyzoite and sexual stage gene
314 expression (6, 19), albeit to a greater extent than does AP2XII-2 depletion. Given the
315 association of AP2XII-2 with AP2IX-4 (12), and the observation that AP2XII-2 depletion
316 appears to cause a milder version of the HDAC3 and MORC phenotypes, we propose
317 that AP2XII-2 is likely one of several AP2 family members that bind cooperatively to
318 recruit the HDAC3/MORC to specific genomic loci.

319 On the other hand, the number of reports demonstrating that *Toxoplasma* studies
320 investigating gene regulation using in vitro culture system lack the fidelity of in vivo
321 parasite development (31-33). This is particularly relevant when examining the roles of

322 AP2 family members in gene regulation (33). Notably, a previous report indicating that
323 AP2IX-9 is a repressor of bradyzoite formation was later contradicted using a
324 developmentally competent *Toxoplasma* models (15, 22, 33). Given that we have
325 reported that AP2XII-2 impacts both cell cycle regulation (12) and the expression of
326 sexually committed gene expression, we cannot rule out the possibility that mis-
327 expression of AP2XII-2 may have resulted in 'transcriptional confusion' that impacted
328 tachyzoite cell cycle dynamics. Examining the role that AP2XII-2 plays throughout the
329 complete life cycle stages of *Toxoplasma* development is warranted.

330 The intrinsic factors responsible for regulating *Toxoplasma* sexual development
331 have been understudied due to the lack of amenable systems. This is beginning to
332 change with the pivotal discoveries of the upstream extrinsic signals required to initiate
333 sexual development and the requirement of widespread transcriptional repression to
334 coordinate the process (6, 34). Future work will undoubtedly focus on disentangling the
335 gene regulatory networks responsible for initiating and managing *Toxoplasma* sexual
336 development. Here we have begun unravelling one of the networks responsible for this
337 process by placing the AP2XII-2-directed HDAC3/MORC complex above two genes that
338 function in sexual stages, AP2X-10 and AAH1. In addition to utilizing a candidate-based
339 approach as we have relied on for this study, the recent report highlighting inhibitors of
340 AP2-family member activity may prove yet another tool for interrogating the role of AP2
341 factors in *Toxoplasma* developmental transitions (35).

342

343 **MATERIALS AND METHODS**

344

345 **Parasite culture**

346 Human fibroblast cells (HFFs, ATCC SCRC-104) were maintained in Dulbecco's
347 modified Eagle medium (DMEM; Corning) supplemented with 10% fetal bovine serum
348 (FBS, R&D systems), 100 µg/ml streptomycin and 100 units/ml penicillin as described
349 elsewhere (36). RH and ME49 parasites were cultured in DMEM supplemented with 1%
350 and 5% heat inactivated FBS, respectively, 100 µg/ml streptomycin and 100 units/ml
351 penicillin. Parasites were maintained in humidified incubator at 37°C and 5% CO_2.
352 Transfected and clonal strains were maintained in selection media supplemented with 1
353 µM pyrimethamine or a combination of 25 µg mycophenolic acid and 50 µg xanthine as
354 appropriate. Control of AP2XII-2 expression was achieved by adding either 500 µM of
355 indole-3-acetic acid or an equivalent amount of ethanol vehicle for 24 hours to the
356 culture media before analysis.

357

358 **Generation endogenously tagged AAH1^{MYC} or AAH2^{MYC}**

359 The ME49-TIR1:AP2XII-2^{AID-HA} strain that we generated in a previous study (12)
360 was used as the parental strain for generating dual-tagged AAH1^{MYC} and AAH2^{MYC}
361 parasites. For AAH1, the guide RNA sequence from the pSAG1::CAS9-U6::sgUPRT
362 plasmid (Addgene 54467) (37) was mutagenized to target the stop codon of AAH1. All
363 primers and sequences are listed in supplement (Table S4). A donor repair template
364 with regions of homology to the AAH1 CDS and 3'UTR was made to incorporate the
365 MYC tag and HXGPRT cassette. Parasites were transfected with 25 µg of CAS9
366 plasmid and 25 µg of donor repair template, were cultured with 25 µg mycophenolic
367 acid and 50 µg xanthine for 7-8 days and single clones were isolated by limiting dilution

368 in 96 wells. Isolated single clones were confirmed for C-terminal tagging by PCR of their
369 genomic DNA (Fig. S2)

370 To generate AAH2^{Myc} parasites, specific primers were used to clone ~2 kb of the
371 AAH2 gene into the PacI site of the pLIC-3xMYC-HXGPRT plasmid. 50 µg of the final
372 construct was linearized with NheI restriction endonuclease and transfected into the
373 ME49-TIR1:AP2XII-2^{AID-HA} strain. Transgenic parasites were selected for 7-8 days
374 under drug pressure and subjected to limiting dilution in 96 well plates. Single clones
375 were confirmed for integration of MYC tag at C-terminus (Fig. S2).

376

377 **Western blotting**

378 Parasites growing in confluent HFF cells were mechanically lysed and filtered to
379 remove host cell debris followed by centrifugation. Parasite pellets were lysed in
380 NuPAGE buffer, sonicated, and boiled for 5 minutes. Parasite lysates were centrifuged
381 briefly to remove debris and separated on 4-12% NuPAGE gels (Invitrogen). Separated
382 proteins were transferred to PVDF membrane and blocked in 5% Nonfat dry milk-TBST
383 solution for 1 hour at room temperature. Blocked PVDF membranes were incubated
384 with anti-HA (1:2000, Roche), anti-MYC (1:3000, Cell Signaling) or anti-SAG1 (1:5000,
385 ThermoFisher) antibodies in blocking buffer at 4°C overnight with gentle shaking.
386 Membranes were washed with TBST and incubated with HRP-conjugated anti-rat or
387 anti-mouse (1:2000; GE healthcare) for 1 hour at room temperature. After washing with
388 TBST, membranes were developed with SuperSignal West Femto substrate
389 (ThermoFisher).

390

391 **Immunofluorescence assay**

392 Parasites growing in HFF monolayers were fixed in 4% paraformaldehyde
393 solution for 15 minutes at room temperature followed by washing with phosphate
394 buffered saline (PBS). Fixed cells were permeabilized and blocked with blocking buffer
395 (3% BSA + 0.2% Triton X-100 in PBS) for 1 h. Cells were incubated with primary
396 antibodies in blocking buffer at 4°C temperature overnight. Cells were washed with PBS
397 and finally incubated with DAPI (1:1000) and Alexa fluor secondary antibodies coupled
398 with desired fluorophore for 1 hour at room temperature. Cells were washed and
399 mounted with Prolong Gold anti-fade reagent (Invitrogen) before analysis with a Leica
400 DMI6000 B inverted microscope. Dilutions for antibodies used for IFA are as follows:
401 Rabbit α-HA (1:2000, Sigma, H6908), Mouse mAb α-MYC (1:1000, Cell signaling,
402 9B11), Rabbit α-MYC (1:2000, ThermoFisher, PA1-981) and Mouse mAb 5F4 (1:5000,
403 F1B ATPase, a gift from Peter Bradley), Alexa Fluor 488/594 secondary antibodies
404 (1:2000, ThermoFisher) were used as appropriate.

405

406 **RNA sequencing**

407 Parasites were allowed to invade confluent HFF monolayers for 24 h. Infected
408 HFF monolayers were scraped, and syringe lysed with 23-gauge needle to release
409 intracellular parasites and passed through a 3 μM filter. Filtered parasites were
410 centrifuged at 300 x *g* for 15 minutes and DMEM media was removed to isolate the
411 parasite pellet. The parasite pellet was resuspended in 1 x PBS and centrifuged at 300
412 x g for 15 minutes, twice. Total RNA was extracted with TRIzol reagent (Invitrogen) as
413 per manufacturer's protocol and measured by Nanodrop. RNAseq libraries were

414 prepared from polyA-purified mRNA by Azenta using standard Illumina protocols.
415 Libraries were sequenced PE x 150bp.
416
417 **RNAseq data analysis**
418 RNAseq read data generated from either the RH or the ME49 genetic
419 background were aligned to the ME49 reference sequence (v52) with hisat2 using
420 default settings (38). Differential gene expression was conducted with DESeq2 using
421 default settings (39). Raw sequencing data and processed files generated in this study
422 are available at GEO GSE217226 and data pertaining to HDAC3 and MORC
423 impairment (6) were obtained from GEO GSE136123.
424
425 **CUT&Tag assay**
426 Chromatin occupancy for ME49^{TIR1} parasites expressing AP2XII-2^{AID-HA} was
427 performed by CUT&Tag profiling (14). Briefly, 2x10^{7} intracellular tachyzoites were
428 syringe lysed 24 hours post invasion to release fresh parasites. Parasites were
429 centrifuged at 600 x *g* for 10 minutes at room temperature. Parasite pellets were then
430 processed as per the manufacturer's protocol (CUT&Tag-IT™ Assay Kit, Anti-Rabbit,
431 Active motif, Cat no. 53160). Libraries were sequenced by Azenta at PE 2x150 bp.
432
433 **Chromatin occupancy data analysis**
434 Sequencing data was aligned to the ME49 genome (v52) with bowtie2 (40)
435 allowing for mate dovetailing. Peaks were called with MACS2 using default settings
436 (41). Peak annotation was performed with Homer using a 2kb cutoff distance (42). Peak

437 overlap was conducted with bedtools overlap function (43). AP2XII-2 data was
438 deposited at GEO GSE217220 and raw data pertaining to ChIPseq of MORC and
439 HDAC3 (6) were obtained from GEO GSE136060.
440
441
442
443 **ACKNOWLEDGEMENTS**
444
445 The authors would like to thank Dr. Peter Bradley for the F_1B ATPase antibody, Dr. Vicki
446 Jeffers for technical advice related to CUT&Tag, and members of the Sullivan lab and
447 Biology of Intracellular Pathogens group at the IU School of Medicine for helpful
448 discussions. This research was supported by National Institutes of Health grants
449 AI124682 (M.W.W.) and AI152583 (W.J.S.). The funders had no role in study design,
450 data collection and interpretation, or the decision to submit the work for publication.
451
452 **REFERENCES**
453 1. Montoya JG, Liesenfeld O. 2004. Toxoplasmosis. Lancet 363:1965-76.
454 2. Jeffers V, Tampaki Z, Kim K, Sullivan WJ, Jr. 2018. A latent ability to persist:
455 differentiation in Toxoplasma gondii. Cell Mol Life Sci 75:2355-2373.
456 3. Sullivan WJ, Jr., Hakimi MA. 2006. Histone mediated gene activation in
457 Toxoplasma gondii. Mol Biochem Parasitol 148:109-16.
458 4. Kim K. 2018. The Epigenome, Cell Cycle, and Development in Toxoplasma.
459 Annu Rev Microbiol 72:479-499.

460 5. Harris MT, Jeffers V, Martynowicz J, True JD, Mosley AL, Sullivan WJ, Jr. 2019.
461 A novel GCN5b lysine acetyltransferase complex associates with distinct
462 transcription factors in the protozoan parasite Toxoplasma gondii. Mol Biochem
463 Parasitol 232:111203.
464 6. Farhat DC, Swale C, Dard C, Cannella D, Ortet P, Barakat M, Sindikubwabo F,
465 Belmudes L, De Bock PJ, Couté Y, Bougdour A, Hakimi MA. 2020. A MORC-
466 driven transcriptional switch controls Toxoplasma developmental trajectories and
467 sexual commitment. Nat Microbiol 5:570-583.
468 7. White MW, Radke JR, Radke JB. 2014. Toxoplasma development - turn the
469 switch on or off? Cell Microbiol 16:466-72.
470 8. Álvarez García G, Davidson R, Jokelainen P, Klevar S, Spano F, Seeber F.
471 2021. Identification of Oocyst-Driven Toxoplasma gondii Infections in Humans
472 and Animals through Stage-Specific Serology-Current Status and Future
473 Perspectives. Microorganisms 9.
474 9. Dubey JP. 2021. Outbreaks of clinical toxoplasmosis in humans: five decades of
475 personal experience, perspectives and lessons learned. Parasit Vectors 14:263.
476 10. Attias M, Teixeira DE, Benchimol M, Vommaro RC, Crepaldi PH, De Souza W.
477 2020. The life-cycle of Toxoplasma gondii reviewed using animations. Parasit
478 Vectors 13:588.
479 11. Zhu S, Shapiro K, VanWormer E. 2022. Dynamics and epidemiology of
480 Toxoplasma gondii oocyst shedding in domestic and wild felids. Transbound
481 Emerg Dis 69:2412-2423.

482 12. Srivastava S, White MW, Sullivan WJ, Jr. 2020. Toxoplasma gondii AP2XII-2
483 Contributes to Proper Progression through S-Phase of the Cell Cycle. mSphere
484 5.
485 13. Huang S, Holmes MJ, Radke JB, Hong DP, Liu TK, White MW, Sullivan WJ, Jr.
486 2017. Toxoplasma gondii AP2IX-4 Regulates Gene Expression during Bradyzoite
487 Development. mSphere 2.
488 14. Kaya-Okur HS, Wu SJ, Codomo CA, Pledger ES, Bryson TD, Henikoff JG,
489 Ahmad K, Henikoff S. 2019. CUT&Tag for efficient epigenomic profiling of small
490 samples and single cells. Nat Commun 10:1930.
491 15. Radke JB, Lucas O, De Silva EK, Ma Y, Sullivan WJ, Jr., Weiss LM, Llinas M,
492 White MW. 2013. ApiAP2 transcription factor restricts development of the
493 Toxoplasma tissue cyst. Proc Natl Acad Sci U S A 110:6871-6.
494 16. Campbell TL, De Silva EK, Olszewski KL, Elemento O, Llinás M. 2010.
495 Identification and genome-wide prediction of DNA binding specificities for the
496 ApiAP2 family of regulators from the malaria parasite. PLoS Pathog 6:e1001165.
497 17. Behnke MS, Wootton JC, Lehmann MM, Radke JB, Lucas O, Nawas J, Sibley
498 LD, White MW. 2010. Coordinated progression through two subtranscriptomes
499 underlies the tachyzoite cycle of Toxoplasma gondii. PLoS One 5:e12354.
500 18. Harb OS, Roos DS. 2020. ToxoDB: Functional Genomics Resource for
501 Toxoplasma and Related Organisms. Methods Mol Biol 2071:27-47.
502 19. Bougdour A, Maubon D, Baldacci P, Ortet P, Bastien O, Bouillon A, Barale JC,
503 Pelloux H, Ménard R, Hakimi MA. 2009. Drug inhibition of HDAC3 and epigenetic
504 control of differentiation in Apicomplexa parasites. J Exp Med 206:953-66.

505 20. Dubey JP. 2005. Unexpected oocyst shedding by cats fed Toxoplasma gondii
506 tachyzoites: in vivo stage conversion and strain variation. Vet Parasitol 133:289-
507 98.
508 21. Ueno A, Dautu G, Munyaka B, Carmen G, Kobayashi Y, Igarashi M. 2009.
509 Toxoplasma gondii: Identification and characterization of bradyzoite-specific
510 deoxyribose phosphate aldolase-like gene (TgDPA). Exp Parasitol 121:55-63.
511 22. Hong DP, Radke JB, White MW. 2017. Opposing Transcriptional Mechanisms
512 Regulate Toxoplasma Development. mSphere 2.
513 23. Ramakrishnan C, Maier S, Walker RA, Rehrauer H, Joekel DE, Winiger RR,
514 Basso WU, Grigg ME, Hehl AB, Deplazes P, Smith NC. 2019. An experimental
515 genetically attenuated live vaccine to prevent transmission of Toxoplasma gondii
516 by cats. Sci Rep 9:1474.
517 24. Fritz HM, Buchholz KR, Chen X, Durbin-Johnson B, Rocke DM, Conrad PA,
518 Boothroyd JC. 2012. Transcriptomic analysis of toxoplasma development reveals
519 many novel functions and structures specific to sporozoites and oocysts. PLoS
520 One 7:e29998.
521 25. Wang ZT, Verma SK, Dubey JP, Sibley LD. 2017. The aromatic amino acid
522 hydroxylase genes AAH1 and AAH2 in Toxoplasma gondii contribute to
523 transmission in the cat. PLoS Pathog 13:e1006272.
524 26. Wang ZT, Harmon S, O'Malley KL, Sibley LD. 2015. Reassessment of the role of
525 aromatic amino acid hydroxylases and the effect of infection by Toxoplasma
526 gondii on host dopamine. Infect Immun 83:1039-47.

527 27. Xia J, Venkat A, Bainbridge RE, Reese ML, Le Roch KG, Ay F, Boyle JP. 2021.
528 Third-generation sequencing revises the molecular karyotype for Toxoplasma
529 gondii and identifies emerging copy number variants in sexual recombinants.
530 Genome Res 31:834-851.
531 28. Heredero-Bermejo I, Varberg JM, Charvat R, Jacobs K, Garbuz T, Sullivan WJ,
532 Jr., Arrizabalaga G. 2019. TgDrpC, an atypical dynamin-related protein in
533 Toxoplasma gondii, is associated with vesicular transport factors and parasite
534 division. Mol Microbiol 111:46-64.
535 29. Gaskell EA, Smith JE, Pinney JW, Westhead DR, McConkey GA. 2009. A unique
536 dual activity amino acid hydroxylase in Toxoplasma gondii. PLoS One 4:e4801.
537 30. Waldman BS, Schwarz D, Wadsworth MH, 2nd, Saeij JP, Shalek AK, Lourido S.
538 2020. Identification of a Master Regulator of Differentiation in Toxoplasma. Cell
539 180:359-372.e16.
540 31. Xue Y, Theisen TC, Rastogi S, Ferrel A, Quake SR, Boothroyd JC. 2020. A
541 single-parasite transcriptional atlas of Toxoplasma Gondii reveals novel control of
542 antigen expression. Elife 9.
543 32. Goerner AL, Vizcarra EA, Hong DD, Bergersen KV, Alvarez CA, Talavera MA,
544 Wilson EH, White MW. 2020. An ex vivo model of Toxoplasma
545 recrudescence. bioRxiv doi:10.1101/2020.05.18.101931:2020.05.18.101931.
546 33. Hong DD, Brooks K, Goerner AL, Vizcarra EA, Loges LN, Wilson EH, White MW.
547 2022. Engineering Toxoplasma transgenic tissue cysts. bioRxiv
548 doi:10.1101/2022.07.21.500998:2022.07.21.500998.

549 34. Martorelli Di Genova B, Wilson SK, Dubey JP, Knoll LJ. 2019. Intestinal delta-6-
550 desaturase activity determines host range for Toxoplasma sexual reproduction.
551 PLoS Biol 17:e3000364.
552 35. Russell TJ, De Silva EK, Crowley VM, Shaw-Saliba K, Dube N, Josling G, Pasaje
553 CFA, Kouskoumvekaki I, Panagiotou G, Niles JC, Jacobs-Lorena M, Denise
554 Okafor C, Gamo FJ, Llinás M. 2022. Inhibitors of ApiAP2 protein DNA binding
555 exhibit multistage activity against Plasmodium parasites. PLoS Pathog
556 18:e1010887.
557 36. Roos DS, Donald RG, Morrissette NS, Moulton AL. 1994. Molecular tools for
558 genetic dissection of the protozoan parasite Toxoplasma gondii. Methods Cell
559 Biol 45:27-63.
560 37. Shen B, Brown KM, Lee TD, Sibley LD. 2014. Efficient gene disruption in diverse
561 strains of Toxoplasma gondii using CRISPR/CAS9. mBio 5:e01114-14.
562 38. Kim D, Langmead B, Salzberg SL. 2015. HISAT: a fast spliced aligner with low
563 memory requirements. Nat Methods 12:357-60.
564 39. Love MI, Huber W, Anders S. 2014. Moderated estimation of fold change and
565 dispersion for RNA-seq data with DESeq2. Genome Biol 15:550.
566 40. Langmead B, Salzberg SL. 2012. Fast gapped-read alignment with Bowtie 2. Nat
567 Methods 9:357-9.
568 41. Feng J, Liu T, Qin B, Zhang Y, Liu XS. 2012. Identifying ChIP-seq enrichment
569 using MACS. Nat Protoc 7:1728-40.
570 42. Heinz S, Benner C, Spann N, Bertolino E, Lin YC, Laslo P, Cheng JX, Murre C,
571 Singh H, Glass CK. 2010. Simple combinations of lineage-determining

572 transcription factors prime cis-regulatory elements required for macrophage and
573 B cell identities. Mol Cell 38:576-89.
574 43. Quinlan AR, Hall IM. 2010. BEDTools: a flexible suite of utilities for comparing
575 genomic features. Bioinformatics 26:841-2.
576
577

578 **FIGURE LEGENDS**

579

580 **Figure 1. AP2XII-2 genome occupancy significantly overlaps with HDAC3 and**
581 **MORC.** A) AP2XII-2 genome occupancy along a segment of chromosome VIIA reveals
582 its association at the promoters of several genes. Statistically enriched segments are
583 shown as black bars directly under AP2XII-2 enriched peaks (purple). A similar
584 distribution and enrichment of HDAC3 and MORC is seen in the orange and teal tracks,
585 respectively. B) Genome-wide analysis reveals each member of the transcriptional
586 repression complex associates with the transcriptional start sites (TSS) of genes. C)
587 Venn diagram indicating that the majority of AP2XII-2 enriched peaks fall within those
588 identified for HDAC3 and MORC. D) Venn diagram indicating that the majority genes
589 occupied by AP2XII-2 are also occupied by HDAC3 and MORC.

590

591 **Figure 2. AP2XII-2 depletion leads to relatively little gene dysregulation.** A)
592 Western blots confirming IAA-dependent downregulation of AP2XII-2^{AID-HA} protein in
593 RH^{TIR1} or ME49^{TIR1} parasites after 24 hours incubation with 500 μM IAA in culture
594 media. Blots were probed with anti-SAG1 as a loading control. B-C) MA plot of
595 differential gene expression analysis of AP2XII-2^{AID-HA}-depleted in RH^{TIR1} (B) or
596 ME49^{TIR1} (C) parasites 24 hours after IAA addition. Significantly upregulated genes are
597 colored in blue, downregulated genes in red. Genes of interest for further analysis are
598 noted. D) Diagrams showing overlap of significantly upregulated and downregulated
599 genes in ME49 and RH genetic backgrounds. E) Analysis of AP2XII-2 gene occupancy
600 and directionality of dysregulation that occurs upon AP2XII-2 depletion. F) Meta cell

601 cycle expression analysis of significantly upregulated (blue) and downregulated (red)
602 gene sets that respond to AP2XII-2 depletion. The cell cycle profile of AP2XII-2 is
603 shown in black as a reference.
604
605 **Figure 3. Disentanglement of the aromatic amino acid hydroxylase family of**
606 **genes on chr V.** A) Genomic alignment and syntenic analysis of RH88 and ME49
607 genomes available on ToxoDB.org reveals the correct positioning of unplaced contigs
608 KE139705 and KE139818 into chr V that was missed due to incorrect fusion of AAH1/2
609 genes in the ME49 reference strain. Suggested changes to annotation of AAH1 and
610 AAH2 are based on sequence alignments of 3' flanking regions in both genes across
611 both parasite strains. B) Multiple pairwise alignments of CDS regions that are present in
612 each AAH gene fragment reveals a high degree of identity at the nucleotide level which
613 obfuscates gene calling during differential gene expression analysis. C) Pairwise
614 alignment of 3' flanking regions reveals a clear way to discriminate both AAH1 and
615 AAH2 genes for C-terminal tagging at endogenous loci. D) Outline of AAH-family gene
616 fragments available in ME49 reference strain. Missing fragments on either 5' or 3'
617 terminus are stated. Conserved CDS regions that were used for multiple sequence
618 alignment are delimited by dotted line.
619
620 **Figure 4. Depletion of AP2XII-2 causes de-repression of AAH1 gene expression.**
621 A-B) Western blots demonstrating that AAH1 (A) and not AAH2 (B) is expressed upon
622 IAA-induced depletion of AP2XII-2. Both genes were endogenously tagged at their C-
623 termini with MYC epitope tags. Blots were probed with anti-SAG1 as a loading control.

624 C) AAH1 expression is observed in a concentric pattern around the nucleus upon
625 AP2XII-2 depletion. D) AAH1 is expressed in the vicinity of the parasite mitochondrial
626 marker F_1BATPase.
627
628

629 **SUPPLEMENTAL FIGURE LEGENDS**

630

631 **Figure S1. Re-analysis of transcriptomic changes that occur upon impairment of**
632 **HDAC3/MORC complex.** A-B) Differential gene expression analysis for HDAC3
633 inhibition (A) and IAA-induced MORC depletion (B), each conducted as it was for newly
634 generated AP2XII-2 depletion data.

635

636 **Figure S2. Validation for endogenous tagging of AAH1 and AAH2.** A) AAH1 was
637 endogenously tagged with a MYC epitope tag using a CAS9-assisted approach to
638 facility double homologous recombination as indicated. B) AAH2 was endogenously
639 tagged with a MYC epitope tag using a single crossover approach as indicated. C-D)
640 Diagnostic PCRs checking for correct integration (I) or the unmodified endogenous
641 locus (E) were performed on parental and tagged lines. Specific regions selected for
642 PCR analysis are highlighted in (A) and (B).

643

644

645 **SUPPLEMENTAL TABLE LEGENDS**

646

647 **Table S1. Chromatin-associated regions for AP2XII-2, HDAC3, and MORC as**

648 **revealed by CUT&Tag or ChIPseq.**

649

650 **Table S2. Differential gene expression analysis resulting from AP2XII-2 depletion**

651 **in RH and ME49 backgrounds.**

652

653 **Table S3. Differential gene expression analysis resulting from HDAC3 inhibition**

654 **or MORC depletion.**

655

656 **Table S4. List of primers used in this study.**

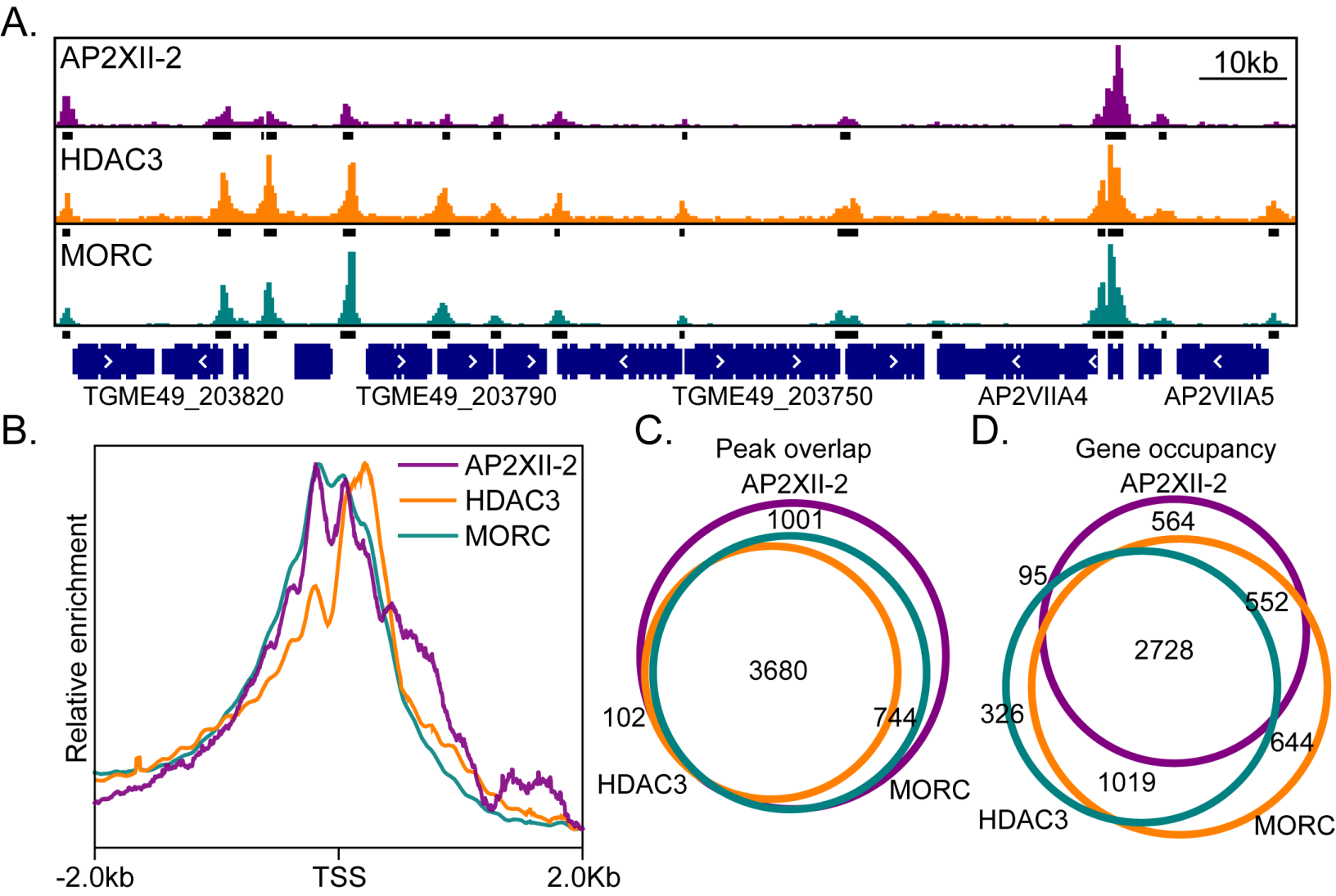
A.
AP2XII-2
10kb
HDAC3
MORC
TGME49_203820
TGME49_203790
TGME49_203750
AP2VIIA4
AP2VIIA5
B.
AP2XII-2
HDAC3
MORC
Relative enrichment
-2.0kb
TSS
2.0Kb
C.
Peak overlap
AP2XII-2
1001
3680
102
744
HDAC3
MORC
D.
Gene occupancy
AP2XII-2
564
95
552
2728
326
644
1019
HDAC3
MORC

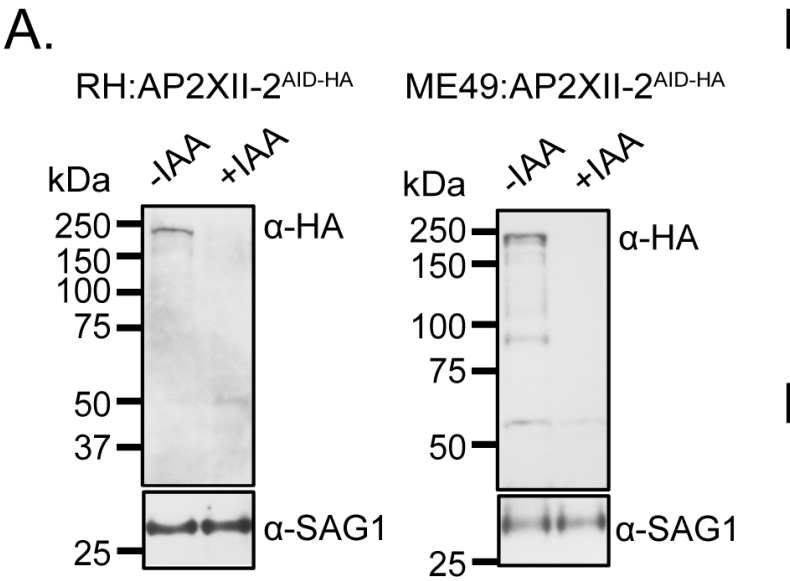
A.
RH:AP2XII-2AID-HA
ME49:AP2XII-2AID-HA
kDa
-IAA
+IAA
250
150
100
75
50
37
25
α-HA
α-SAG1

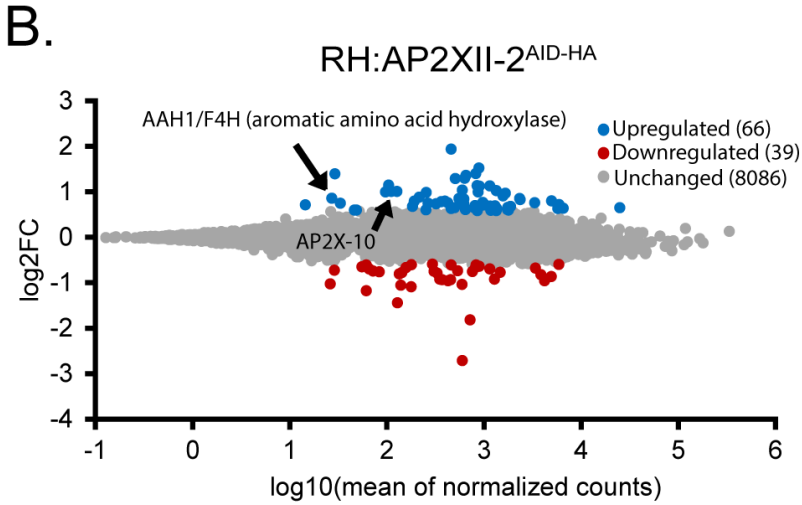
B.
RH:AP2XII-2AID-HA
AAH1/F4H (aromatic amino acid hydroxylase)
AP2X-10
Upregulated (66)
Downregulated (39)
Unchanged (8086)
log2FC
log10(mean of normalized counts)

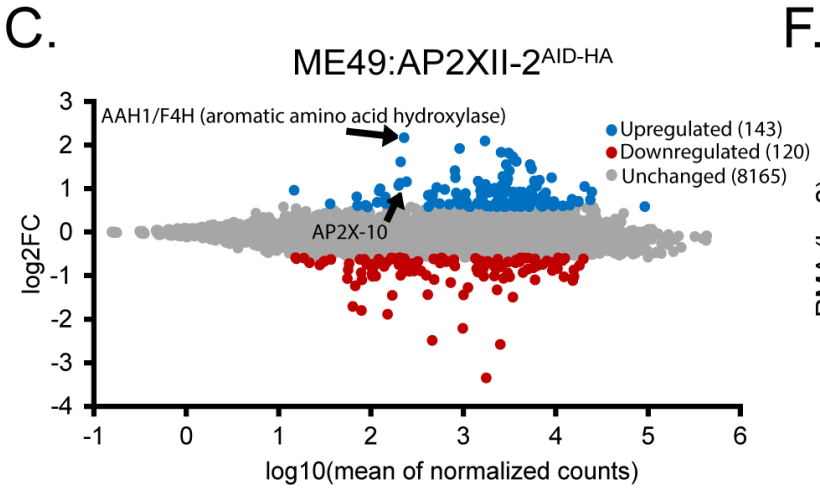
C.
ME49:AP2XII-2AID-HA
AAH1/F4H (aromatic amino acid hydroxylase)
AP2X-10
Upregulated (143)
Downregulated (120)
Unchanged (8165)
log2FC
log10(mean of normalized counts)

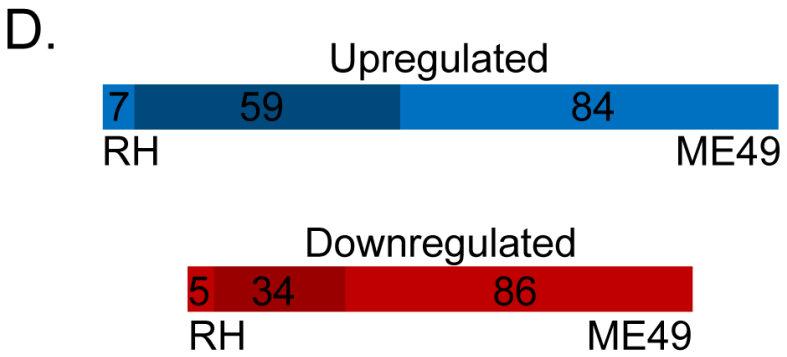
D.
Upregulated
7
59
84
RH
ME49
Downregulated
5
34
86
RH
ME49

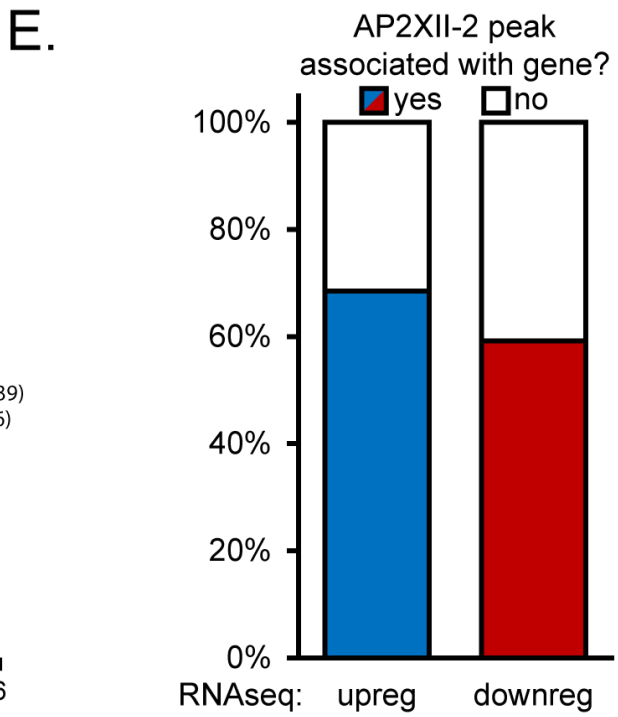
E.
AP2XII-2 peak
associated with gene?
yes
no
100%
80%
60%
40%
20%
0%
RNAseq:
upreg
downreg

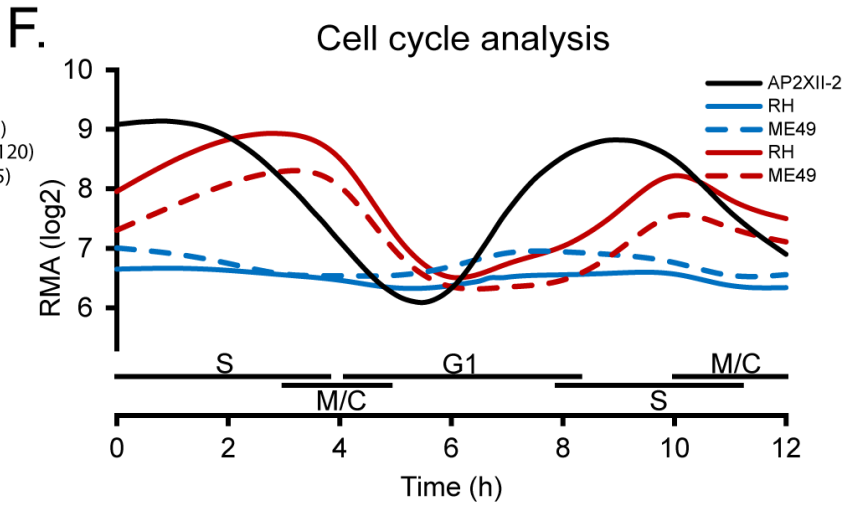
F.
Cell cycle analysis
AP2XII-2
RH
ME49
RH
ME49
RMA (log2)
S
G1
M/C
M/C
S
Time (h)

A

RH88 - long read genome assembly

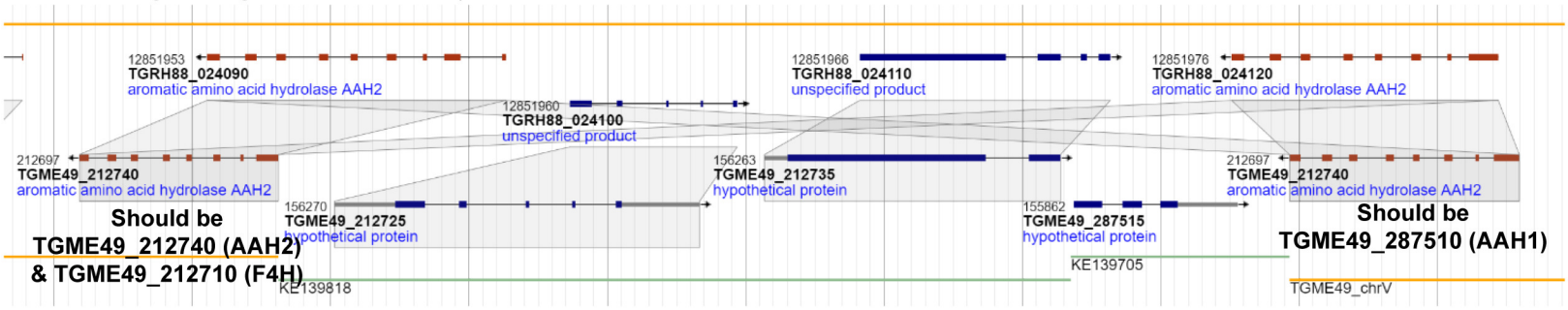

ME49 Reference Genome - short read assembly missing insert between incorrectly fused AAH2 gene

B

% identity at nucleotide level in aligned CDS

99.4% < TGME49_287510 (AAH1) > 99.6%
TGME49_212710 (F4H)
TGME49_212740 (AAH2) > 99.8%

C

% identity at nucleotide level in aligned 3'UTRs

TGME49_287510 (AAH1)
TGME49_212740 (AAH2) > 42.2%

D

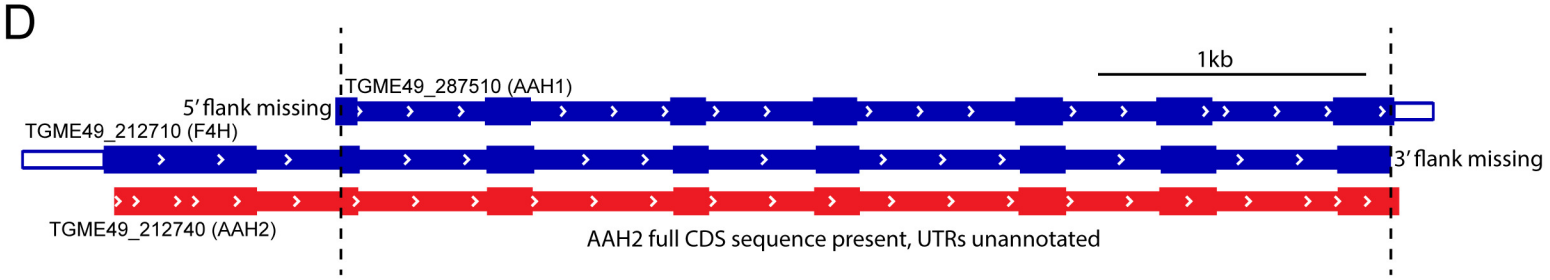

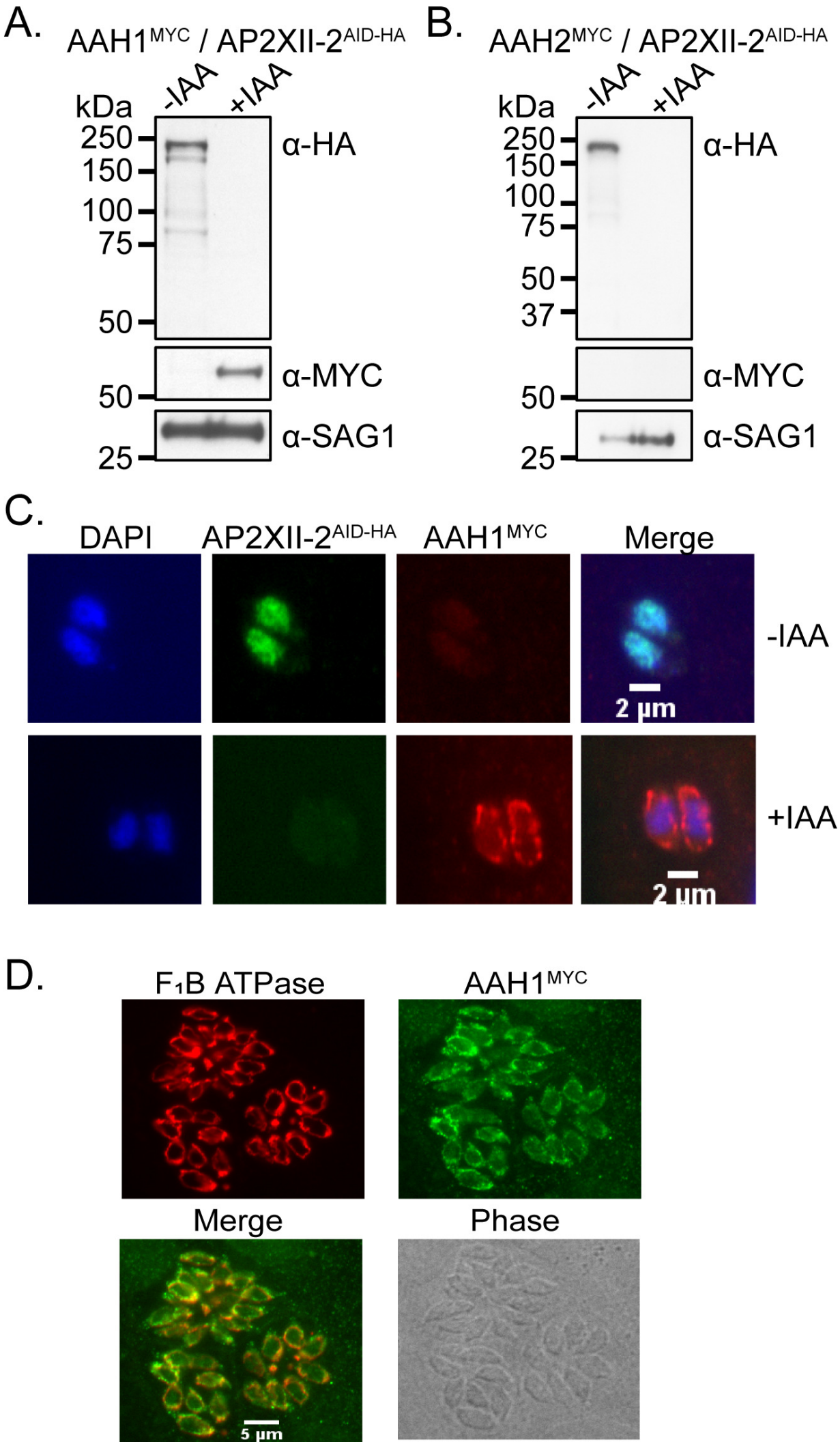
A.
AAH1MYC / AP2XII-2AID-HA
-IAA
+IAA
kDa
250
150
100
75
50
α-HA
50
α-MYC
25
α-SAG1
B.
AAH2MYC / AP2XII-2AID-HA
-IAA
+IAA
kDa
250
150
100
75
50
37
α-HA
50
α-MYC
25
α-SAG1
C.
DAPI
AP2XII-2AID-HA
AAH1MYC
Merge
-IAA
2 µm
+IAA
2 µm
D.
F1B ATPase
AAH1MYC
Merge
Phase
5 µm